Amino Acids (2011) 40:981–989
DOI 10.1007/s00726-010-0725-x

ORIGINAL ARTICLE

Biophysical characterization of recombinant HIV-1 subtype C virus infectivity factor

Daniela Gallerano · Siva Charan Devanaboyina · Ines Swoboda · Birgit Linhart · Irene Mittermann · Walter Keller · Rudolf Valenta

Received: 28 May 2010 / Accepted: 11 August 2010 / Published online: 31 August 2010

Abstract HIV-1 virus infectivity factor (Vif) is one of the four accessory proteins that are characteristic of primate lentiviruses and critically required for the infection of host cells. Vif plays a key role in replication and transmission of the virus in non-permissive cells, such as primary T cells and macrophages. Using co-precipitation and co-fractionation techniques, evidence has been provided that Vif interacts with a variety of host proteins, such as the cytidine deaminases APOBEC3G and 3F, the Cullin5/EloBC ubiquitin–ligase complex, Fyn and Hck tyrosine kinases, as well as with viral components, such as the immature Gag precursor and viral RNA. We report on the expression, purification and molecular characterization of a folded recombinant subtype C Vif. Vif was expressed in *E. coli* with a C-terminal hexahistidine tag and purified by nickel affinity chromatography. We obtained approximately 5 mg protein per liter of bacterial culture, with a purity >95%. The expected molecular mass of 23.7 kDa was confirmed by mass spectrometry. Although dynamic light scattering and small angle X-ray scattering measurements revealed the presence of high molecular weight aggregates in the protein preparation, circular dichroism analysis showed that the protein contains mainly folded β-sheet elements and exhibits remarkable thermal stability ($T_m > 95$°C). Recombinant Vif may be used as a tool to study its biological functions and tertiary structure, as well as for the development of diagnostic, therapeutic and preventive strategies for HIV-1 infections.

Keywords HIV · Virus infectivity factor (Vif) · *E.coli* expression · Circular dichroism · Thermal stability

Abbreviations

HIV	Human immunodeficiency virus
Vif	Virus infectivity factor
rVif	Recombinant virus infectivity factor

Introduction

HIV infections are a major health threat (Taylor and Hammer 2008). The pathogenesis of HIV infection relies on the virus ability to manipulate and evade from the immune system. In this study, we characterize the virus infectivity factor (Vif) which is one of the four accessory proteins that are characteristic of primate lentiviruses and essential in counteracting host defenses (Malim and Emerman 2008). Vif has been shown to block incorporation of the cellular restriction factor APOBEC3G (apolipoprotein-B-messenger-RNA-editing enzyme, catalytic polypeptide-like 3G) and other components of this cytidine deaminase family in virion particles budding from "non-permissive" cells, such as T cells and macrophages. This leads to the

D. Gallerano · I. Swoboda · B. Linhart · I. Mittermann · R. Valenta (✉)
Division of Immunopathology, Department of Pathophysiology and Allergy Research, Center of Pathophysiology, Infectiology and Immunology, Medical University of Vienna, 1090 Vienna, Austria
e-mail: rudolf.valenta@meduniwien.ac.at

S. C. Devanaboyina · W. Keller
Institute of Molecular Biosciences, Structural Biology, Karl-Franzens-University Graz, 8010 Graz, Austria

I. Swoboda · R. Valenta
Christian Doppler Laboratory for Allergy Research, Division of Immunopathology, Department of Pathophysiology and Allergy Research, Center of Pathophysiology, Infectiology and Immunology, Medical University of Vienna, 1090 Vienna, Austria

inhibition of APOBEC3-mediated anti-HIV effect and a subsequent enhancement of viral infectivity (Goila-Gaur and Strebel 2008; Holmes et al. 2007; Malim and Emerman 2008; Sheehy et al. 2002).

Despite the importance of Vif for the pathogenesis of HIV infections, as yet no folded recombinant Vif has been produced and only few structural data regarding Vif are available. The crystal structure of a synthetic Vif peptide comprising amino acid 139–176 of the Vif protein with the E3-ubiquitin ligase complex has been determined (Stanley et al. 2008). Furthermore, CD and NMR studies have been performed for a chemically synthesized C-terminal Vif peptide (Reingewertz et al. 2009). Mass spectrometry analysis of cross-linked Vif indicated that it forms oligomers (Auclair et al. 2007).

To date, the great majority of studies regarding Vif used constructs based on subtype-B derived sequences (Bouyac et al. 1997; Feng et al. 2004; Goncalves et al. 1994; Nguyen et al. 2004; Yang et al. 1996). However, a rapid spread of HIV-1 subtype C has been reported in the last decade. It has become the most prevalent subtype causing up to 47% of global infections and 94% of infections in Southern Africa, where the highest rates of affected adults are reported (Nkolola and Essex 2006; UNAIDS 2008). HIV-1 subtype C has also received attention because of several peculiar features, such as high viral loads, preferential CCR5 co-receptor usage and specific antigenic properties (Kothe et al. 2006; Nkolola and Essex 2006; Taylor and Hammer 2008).

Therefore, we focused on the expression, purification and molecular characterization of a recombinant HIV-1 Vif (rVif) based on the South African subtype C reference strain (Leitner et al. 2005). Particular attention was given to optimize the expression and purification strategies to obtain a soluble and folded Vif protein. The recombinant protein was then characterized regarding its biophysical features by studying its structure, stability and aggregation behavior. Recombinant folded Vif may now be used to shed light onto its three-dimensional structure and its role in the pathogenesis of HIV infections, as well as for the development of diagnostic and therapeutic tools.

Materials and methods

Plasmid construct

The cDNA sequence used for the generation of recombinant subtype C Vif was derived from the South African HIV-1 subtype C reference strain: isolate 04ZA SK164B1 (Los Alamos HIV sequence database accession no. AY772699, http://www.hiv.lanl.gov/). The synthetic gene encoded the Vif gene followed by a hexa histidine tag and a STOP codon at the 3′ end. It was codon-optimized for the expression in *E. coli* and inserted into plasmid pET17b (Novagen, Madison, WI, USA) using 5′*Nde*I and 3′*Eco*RI unique restriction sites (ATG:biosynthetics, Merzhausen, Germany). The construct's identity was verified by restriction analysis with *Nde*I and *Eco*RI, as well as by DNA sequencing (ATG:biosynthetics).

Expression of recombinant Vif in *E. coli*

The pET17b plasmid containing the Vif cDNA was transformed into *E. coli* BL21-Gold (DE3) strain (Stratagene, La Jolla, CA, USA). Cultures were grown from single colonies in LB medium supplemented with 100 mg/l ampicillin at 37°C to an $OD_{600} = 0.5$. The expression of the recombinant protein was induced by addition of 0.5 mM isopropyl-β-thiogalactopyranoside (IPTG). After 4-h incubation at 37°C, cells were harvested by centrifugation (3,500×*g*, 15 min, 4°C) and stored at −20°C.

Time-course analysis of protein expression

The optimal induction period was determined by analyzing 1 ml aliquots taken from cultures before and 2, 3, or 4 h after addition of 0.5 mM IPTG. After centrifugation (10,000×*g*, 5 min, 4°C), cells were re-suspended in a 1:1 mixture of distilled H_2O and 4× Laemmli buffer and analyzed on a 12.5% SDS-PAGE (Laemmli 1970). For rVif detection, cellular extracts were blotted onto nitrocellulose (Whatman, Dassel, Germany) (Towbin et al. 1979). The membrane was then exposed to a monoclonal mouse anti-His-tag antibody (0.2 µg/ml) (Dianova, Hamburg, Germany) and bound antibodies were detected with an alkaline phosphatase-coupled rabbit anti-mouse IgG antibody (0.5 µg/ml) (BD-Biosciences, Erembodegem, Belgium).

Analysis of rVif solubility

Five 1-ml culture aliquots were taken after 4-h induction with 0.5 mM IPTG. Cells were harvested by centrifugation (10,000×*g*, 5 min, 4°C) and stored at −20°C. Cell pellets were lysed by three cycles of freezing and thawing and re-suspended in 500 µl of the following lysis buffers: *Buffer 1* 10 mM Tris–HCl, pH 7.5; *Buffer 2* 10 mM Tris–HCl, 200 mM NaCl, pH 7.5; *Buffer 3* 10 mM Tris–HCl, 0.1% Triton X-100, pH 7.5; *Buffer 4* 10 mM Tris–HCl, 8 M urea, pH 7.5; *Buffer 5* 100 mM Tris–HCl, 6 M guanidiniumhydrochloride (GndHCl), 10 mM β-mercaptoethanol, pH 8.3. After vortexing and incubating for 10 min on ice, lysates were centrifuged at 10,000×*g* for 5 min at 4°C and pellets were re-suspended in 500 µl 4× Laemmli buffer. Soluble and insoluble fractions of each lysis approach were analyzed by 12.5% SDS-PAGE.

Purification of recombinant Vif

Recombinant Vif was purified from the insoluble fraction of a 250 ml expression culture using an inclusion body preparation protocol. The purification steps are as shown in Fig. 1.

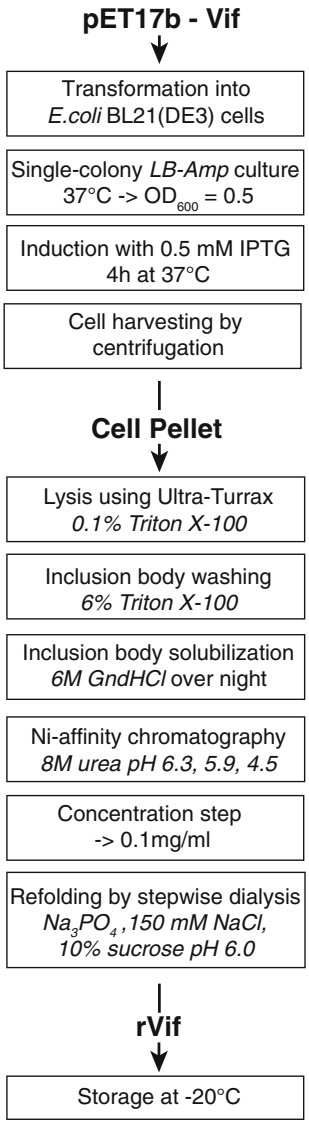

Fig. 1 Flowchart of rVif expression and purification. The optimized expression and purification protocol are represented schematically. Buffers are indicated in *italics*. *LB-Amp* LB-medium supplemented with 100 mg/l ampicillin; *0.1% Triton X-100* 25 mM imidazole, 0.1% Triton X-100, pH 7.4; *6% Triton X-100* 6% Triton X-100, 60 mM EDTA, 150 mM NaCl, pH 7.0; *6 M GndHCl* 6 M GndHCl, 100 mM Tris–HCl, 10 mM β-mercaptoethanol, pH 8.3; *8 M urea* 8 M urea, 100 mM NaH_2PO_4, 10 mM Tris–HCl, pH 6.3, 5.9, 4.5; *Na_3PO_4* (10 mM NaH_2PO_4), *150 mM NaCl, 10% sucrose, pH 6.0* Dialysis buffer 100 mM NaH_2PO_4, 10 mM Tris–HCl, 150 mM NaCl, 10% sucrose, pH 6.0 with decreasing urea concentrations (6/4/2/1/0.5 M); final buffer 20 mM Na-phosphate, 150 mM NaCl, 10% sucrose, pH 6.0

The cell pellet was thawed on ice, re-suspended in 25 mM imidazole, 0.1% Triton X-100, pH 7.4 and lysed using an Ultra-Turrax (Janke & Kunkel–IKA Labortechnik, Staufen, Germany). The lysate was incubated for 30 min with 10 μg/ml DNaseI at room temperature. After adding 6% Triton X-100, 60 mM EDTA, 1.5 M NaCl, pH 7.0, the lysate was centrifuged at 15,000×*g* for 20 min at 4°C. The pellet was washed again in 6% Triton X-100- and 0.1% Triton X-100- based buffers. To solubilize the inclusion body fraction the resulting pellet was dissolved in 6 M GndHCl, 100 mM Tris–HCl, 10 mM β-mercaptoethanol, pH 8.3 overnight at room temperature and the cellular debris was removed by subsequent centrifugation at 15000×*g*, 20 min, 4°C. Purification of rVif was achieved by Ni-affinity chromatography under denaturing conditions (Qiagen, Hilden, Germany). A protein–resin complex was formed in a batch procedure (3 h incubation time) and subsequently loaded onto a polypropylene column (Qiagen, Hilden, Germany). After washing twice with 8 M urea, 100 mM NaH_2PO_4, 10 mM Tris–HCl, pH 6.3, rVif was eluted in the same buffer at pH 5.9 and pH 4.5. Elution fractions containing rVif were pooled and concentrated to 0.1 mg/ml in an Amicon Ultra-15 centrifugal filter device, MWCO 10000 (Millipore, Billerica, MA). Urea was removed by stepwise dialysis against a 100-fold volume of 100 mM NaH_2PO_4, 10 mM Tris–HCl, 150 mM NaCl, pH 6.0 with decreasing urea concentrations (6, 4, 2, 1 and 0.5 M), supplemented either with 10% sucrose or 20% glycerol. The refolded sample was dialyzed against the final buffer containing 10 mM Na-phosphate pH 6.0, 150 mM NaCl, 10% sucrose or 20% glycerol once overnight and then for 3 h, to assure complete removal of urea. All dialysis steps were carried out at 4°C for at least 3 h, using a 3500 MWCO Spectra/Por 3 regenerated cellulose membrane tube (Spectrum Laboratories Inc., Rancho Dominguez, CA).

For on-column-refolding during Ni-affinity chromatography, the matrix-protein solution was washed with 8 M urea, 100 mM NaH_2PO_4, 10 mM Tris–HCl, 20% glycerol, pH 6.3 and then with 500 mM NaCl, 20 mM Tris–HCl, 20% glycerol, pH 8.0 with decreasing urea concentrations (6, 4, 2, 1 and 0 M). Elution was carried out under native conditions with 50 mM NaH_2PO_4, 300 mM NaCl and 250 mM imidazole.

The extent of rVif precipitation during dialysis was investigated in 10 mM Na-phosphate, pH 6.0 for the following compounds: 5–150 mM NaCl; 10–20% glycerol; 20% EtOH; 10% sucrose; 50 mM glycine, 5 mM EDTA; 50 mM glycine, 5 mM EDTA, 0.005% Tween; 5–50 μM $ZnCl_2$.

For circular dichroism (CD) analyses, NaCl was eliminated from the sample by stepwise dialysis against 10 mM Na-phosphate, pH 6.0 containing decreasing salt

concentrations (150, 75, 0 mM). Again, all dialysis steps were done at 4°C for at least 3 h.

The removal of urea by ultrafiltration was also performed by ultrafiltration on a VivaSpin column, MW 3,500 (VIVASCIENCE, Hannover, Germany). The sample was first concentrated by centrifugation and then washed twice with 10 mM Na-phosphate, 20% glycerol at pH 6.0.

Sample concentration after dialysis was achieved using an Amicon Ultra-15 centrifugal filter device, MWCO 10000 (Millipore).

The purity of the recombinant protein was judged by 12.5% SDS-PAGE and Coomassie Brilliant Blue staining. Protein concentration was determined with a Micro BCA kit (Novagen, Darmstadt, Germany), using bovine serum albumin (BSA) as a standard, as well as by measuring the absorbance at 280 nm, considering an extinction coefficient of 56045 and an OD_{280} for 1 mg/ml of 2.35, as predicted by ProtParam (Gasteiger et al. 2005) on the Expasy proteomics server (http://www.expasy.ch/tools/).

Matrix-assisted laser desorption and ionization time-of-flight (MALDI-TOF) mass spectrometry

Laser desorption mass spectra were acquired on a Microflex MALDI-TOF mass spectrometer (Bruker Daltonics Inc, Billerica, MA). Samples were dialyzed against 10 mM Na-phosphate, pH 6.0 and dissolved in 10% acetonitrile, 0.2% trifluoroacetic acid. For sample preparation a 1:1 mixture of protein and matrix solution (sinapinic acid dissolved in 50% acetonitrile, 0.1% trifluoroacetic acid) was deposited onto a target and air dried. Acquired spectra were analyzed with the Bruker Daltonics FlexAnalysis software.

Circular dichroism analysis

Circular dichroism (CD) spectra were measured on a Jasco J-810 spectropolarimeter (Japan Spectroscopic Co., Tokyo, Japan) using a 0.2-cm path length rectangular quartz cuvette equilibrated at 25°C. Samples were dissolved in 10 mM Na-phosphate, pH 6.0 at a concentration of 0.1 mg/ml. Spectra were recorded at 25°C between 190 and 260 nm, with a resolution of 0.5 nm, at a scan speed of 50 nm/min and resulted from averaging three scans. The final spectra were baseline corrected by subtracting the corresponding buffer spectra obtained under identical conditions. The results were expressed as mean residue ellipticity (Θ) at a given wavelength. Temperature scans were performed according to a step-scan procedure, where the samples were heated from 25 to 95°C, with a heat rate of 2°C/min and cooled back to 25°C at the same rate. Three spectra were recorded every 5°C and averaged. The secondary structure content of rVif was calculated using the secondary structure estimation algorithm CDSSTR (Whitmore and Wallace 2004, 2008) with Reference Set number 4, which is optimized exactly for the wavelength range 190–260 nm.

During the thermal denaturation experiment rVif, dissolved in 10 mM Na-phosphate, pH 6.0, at a concentration of 0.1 mg/ml, was heated 10 min at 95°C on a separate thermomixer (Eppendorf, Hamburg, Germany). CD spectra were recorded immediately after heating as described above.

Size exclusion chromatography

Aliquots of 100 µl of rVif, in 20 mM Na-phosphate, 150 mM NaCl, 10% sucrose, pH 6.0 at a concentration of 0.3 mg/ml, were loaded onto a Superdex-200 30/10 column pre-equilibrated in the same buffer. A flow rate of 0.5 ml/min was used to perform the chromatography run.

Dynamic light scattering

Dynamic light scattering (DLS) measurements were performed on a DynaPro Molecular Sizing Instrument (Protein Solutions, USA), equipped with a Peltier-thermostated cell holder and a 0.45µl micro-cuvette. Measurements were performed with 50% laser power at a wavelength of 830 nm and a temperature of 20°C. Protein samples, prepared in 20 mM Na-phosphate, 150 mM NaCl, 10% sucrose, pH 6.0 at a concentration of 0.3 mg/ml, were centrifuged for 15 min at $15000\times g$ and passed through a 0.22-µm filter before measurement. Scattered light intensity was recorded every 10 s and 15 measurements with sum of squares (SOS) values <100 and a base line of ~ 1.0 were taken. Based on these measurements, translational diffusion coefficients (D) were estimated from the autocorrelation function. Diffusion coefficients were used to calculate hydrodynamic radii (R_h).

Small angle X-ray scattering

Small angle scattering measurements were performed at the small angle X-ray scattering (SAXS) beamline X33 at the European Molecular Biology Laboratory Outstation, DESY. A MAR345 Image Plate detector (Marresearch, Norderstedt, Germany) was used at a sample-detector distance of 2.7 m and a wavelength of 0.15 nm. Protein samples were prepared in 20 mM Na-phosphate, 150 mM NaCl, 20% glycerol, pH 6.0 and data were collected at protein concentrations of 1.36, 0.67 and 0.31 mg/ml. Blank measurements using the identical buffer were taken before and after each protein measurement. BSA at a concentration of 4.5 mg/ml was used as a standard. The data were processed using the software PRIMUS (Konarev et al. 2003). The pair-distribution function ($p(r)$) was calculated

with the program GNOM (Svergun 1992) using the scattering data of the sample with the highest protein concentration (1.36 mg/ml). The resulting $p(r)$ was used to determine the maximum particle size (D_{max}).

Programs for analysis of protein features

Protein predictions were carried out using the amino acid sequence of HIV-1 subtype C isolate 04ZA SK164B1 (Los Alamos HIV sequence database accession no. AY772699, http://www.hiv.lanl.gov/) as input for the following estimation programs: ProtParam on the Expasy proteomic server (http://www.expasy.ch.tools/) for general protein properties; PsiPred (Bryson et al. 2005; Jones 1999) for secondary structure predictions (bioinf.cs.ucl.ac.uk/psipred).

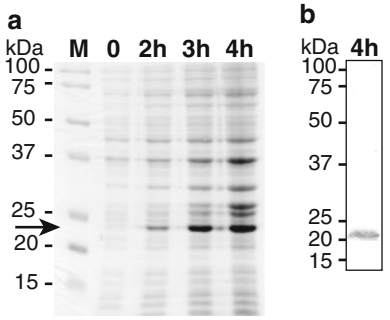

Fig. 2 Time-course analysis of rVif expression. **a** Coomassie-stained gel containing culture aliquots obtained before (0), 2, 3 and 4 h after induction with 0.5 mM IPTG. Molecular weights (kDa) are indicated on the *left margin*, the *arrow* shows rVif at 23.7 kDa. **b** Nitrocellulose-blotted rVif is visualized at 23.7 kDa with a monoclonal mouse anti-His-tag antibody

Results and discussion

E. coli expression and purification of recombinant Vif

Vif is a key protein involved in the pathogenesis of HIV infection (Malim and Emerman 2008). It inhibits the antiviral effect of APOBEC3 and thus enhances viral infectivity. To the best of our knowledge, this study is the first to report the expression and purification of a folded recombinant Vif protein. We expressed Vif of the South African HIV-1 subtype C reference strain because this strain is highly prevalent in Southern Africa, where the highest rates of HIV infection are reported (Leitner et al. 2005; Nkolola and Essex 2006; UNAIDS 2008). To overcome problems that might be caused by the uncommon lentiviral codon usage (Deml et al. 2001; Haas et al. 1996; Holler et al. 1993), we prepared a synthetic gene encoding for a His-tagged subtype C Vif which was optimized for the expression in *E. coli*.

To maximize the expression yield of rVif, we studied protein expression before and at different time points after induction with IPTG (Fig. 2a). A protein band migrating at 23–24 kDa, which corresponded to the molecular weight of rVif, appeared 2 h after induction. The intensity of this band increased until 4 h post-induction and remained largely unaltered in the further course of expression. Therefore, cells were harvested after 4 h of induction. The identity of rVif was verified using a monoclonal anti-His-tag antibody which reacted specifically with the 23–24 kDa over-expressed protein (Fig. 2b).

Previous studies showed that when Vif was expressed in *E. coli* as a fusion protein with glutathione *S* transferase it could be purified from the soluble fraction (Bouyac et al. 1997), whereas the expression of an N-terminally His-tagged Vif led to its accumulation in *E. coli* inclusion bodies (Yang et al. 1996). Although we used a construct

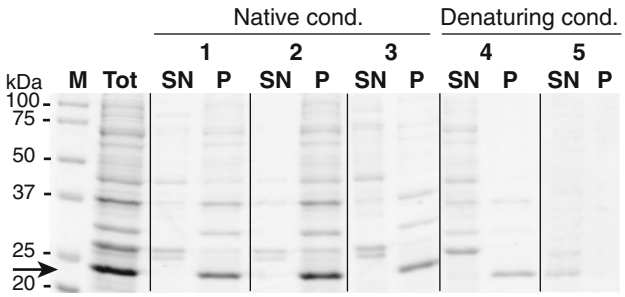

Fig. 3 Analysis of rVif solubility in different buffers. The presence of rVif in supernatant (*SN*) and pellet (*P*) fractions after lysis of *E.coli* in different buffers (1–5) is compared on a Coomassie-stained gel. *Tot E. coli* total proteins before lysis. *Native conditions*: *1* 10 mM Tris–HCl, pH 7.5; *2* 10 mM Tris–HCl, 200 mM NaCl, pH 7.5; *3* 10 mM Tris–HCl, 0.1% Triton X-100, pH 7.5; *Denaturing conditions*: *4* 10 mM Tris–HCl, 8 M urea, pH 7.5; *5* 100 mM Tris–HCl, 6 M GndHCl, 10 mM β-mercaptoethanol, pH 8.3. Molecular weights (kDa) are indicated on the *left margin* and an *arrow* shows rVif at 23.7 kDa

which was codon-optimized for the expression in *E. coli*, the recombinant protein was always found in the insoluble fraction, even when salt or detergents were added (Fig. 3: Buffers 1–3). We could solubilize the protein from inclusion bodies with 6 M GndHCl (Fig. 3; Buffer 5) but not with 8 M urea (Fig. 3; Buffer 4). These data are in agreement with the findings by Yang et al. (1996) who also reported *E. coli*-expressed Vif to be soluble in GndHCl. We then purified His-tagged Vif using a protocol for inclusion body preparation followed by Ni-affinity chromatography. Washing with 8 M urea-based buffer at pH 6.3 allowed to remove other *E. coli* proteins from the lysate-matrix solution and rVif could be eluted in an urea-containing buffer at pH 4.5 (Fig. 4a).

We then developed a protocol for the refolding of rVif. In the first attempt, we removed urea prior to elution using

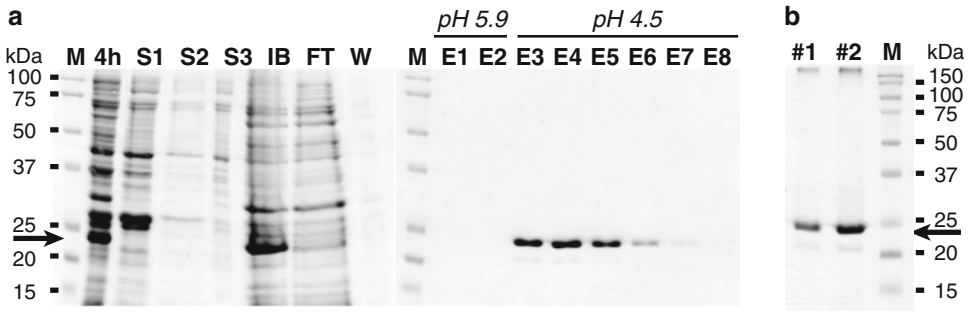

Fig. 4 rVif purification and refolding. **a** Coomassie-stained gel, containing fractions of the different purification steps. 4 h: Four hours after IPTG induction, before lysis; *S1* Supernatant after cell lysis in 25 mM imidazole, 0.1% Triton X-100, pH 7.4, treatment with DNaseI and 6% Triton X-100, 60 mM EDTA, 150 mM NaCl, pH 7.0; *S2* Soluble fraction after washing with 6% Triton X-100, 60 mM EDTA, 1.5 M NaCl, pH 7.0; *S3* Soluble fraction after washing with 25 mM imidazole, 0.1% Triton X-100, pH 7.4. *IB* Inclusion body fraction solubilized in 6 M GndHCl, 100 mM Tris–HCl, 10 mM β-mercaptoethanol, pH 8.3; *FT* Flow through Ni–NTA column. *W* Wash in 8 M urea, 100 mM NaH_2PO_4, 10 mM Tris–HCl, pH 6.3. *E1–2* Eluates at pH 5.9; *E3–8* Eluates at pH 4.5. Molecular weights (kDa) are indicated on the *left margin* and an *arrow* shows rVif at 23.7 kDa. **b** Coomassie-stained gel containing rVif after refolding by stepwise dialysis. The protein is shown at a protein concentration of 0.2 mg/ml (*#1*) and 0.4 mg/ml after concentration by ultrafiltration (*#2*). Molecular weights (kDa) are indicated on the *left margin* and an *arrow* shows rVif at 23.7 kDa

an on-column-refolding process. However, rVif could not be eluted from the Ni–NTA matrix, probably due to the formation of aggregates during the on-column-refolding process (data not shown). In fact, Vifs tendency to form high molecular weight complexes has been reported in previous in vitro and in vivo studies (Auclair et al. 2007; Chiu et al. 2005; Yang et al. 1996, 2001).

To overcome this problem, we eluted rVif keeping the urea concentration high (8 M) and studied various dialysis conditions. Stepwise removal of the denaturing agent was performed next. At urea concentrations below 1 M rVif tended to form visible precipitates. However, this precipitation could be avoided when the protein concentration was kept in the order of 0.1 mg/ml during dialysis and when a pH between 5.5 and 6.5 was used. We further found that the addition of salt, in particular 150 mM NaCl, increased rVifs solubility. Then we tested several co-solvents and additives regarding their ability to prevent protein precipitation. The addition of sucrose or glycerol to 10–20% of the dialysis volume increased the solubility of rVif, whereas the addition of glycine, EtOH or $ZnCl_2$ promoted aggregation (data not shown). We thus succeeded in obtaining soluble rVif by stepwise dialysis against Na-phosphate, 150 mM NaCl and 10% sucrose/20% glycerol by removing urea at pH 6.0. It was even possible to remove NaCl by stepwise dialysis, which was necessary for CD analyses due to the absorbance of Cl^- ions below 200 nm. However, under these conditions, the protein started to precipitate at 4°C (data not shown).

Besides dialysis, ultrafiltration was also tested for the removal of urea. Although no rVif was lost neither during urea elimination nor during the washing steps, the technique displayed poor reproducibility and the presence of urea in the sample preparation could not be totally excluded (data not shown). Therefore, stepwise dialysis was chosen for the removal of denaturing components.

When a sample concentration higher than 0.1 mg/ml of rVif was required (i.e., to perform SAXS and DLS), rVif could be concentrated by ultrafiltration. However, when the protein concentration was increased from 0.1 to 0.4 mg/ml (Fig. 4b), approximately 30% of the sample was lost due to precipitation (data not shown).

The described expression and purification procedure yielded approximately 5 mg rVif per liter of *E. coli* liquid culture grown in incubators, with a purity >95%. We expect that the yield might be strongly increased if fed-batch fermentation procedures are applied.

Recombinant Vif is a folded and highly stable protein

Then we characterized the biophysical features of purified HIV-1 subtype C rVif. Table 1 shows the expected and experimentally confirmed properties of rVif.

We determined the molecular mass of rVif by MALDI-TOF mass spectrometry. A main peak was detected at a mass/charge ratio of 23,802 Da. Minor peaks were observed at 47,526 and in the range of 16,000 Da (Fig. 5). The peak at 23,802 Da corresponded well with the calculated molecular mass for rVif containing the N-terminal methionine (23,667 Da). The peak at 47,526 may result from a rVif dimer and the peaks at 16,000 Da from rVif degradation products which could be detected with the anti-His-tag antibody in certain preparations (data not shown).

To assess whether rVif was folded, we carried out circular dichroism analyses. When analyzed by far-UV CD, rVif showed a minimum at 213–215 nm indicating that the protein contains mainly β-sheet elements (Fig. 6). The rVif

Table 1 Biophysical characterization of Vif

Feature		Predicted, described by	Verified by
Molecular weight (Mw)	23.7 kDa	ProtParam, 1	SDS-PAGE, MALDI-TOF
Isoelectric point (pI)	10.47	ProtParam, 1	–
Secondary structure	β-sheet + α-helical	PsiPred	CD spectroscopy
Quaternary structure	Oligomeric	1, 2–4	DLS, SAXS
Thermal stability	$T_m > 95°C$	–	CD spectroscopy

1,2 (Yang et al. 1996, 2001); 3 (Chiu et al. 2005); 4 (Auclair et al. 2007)

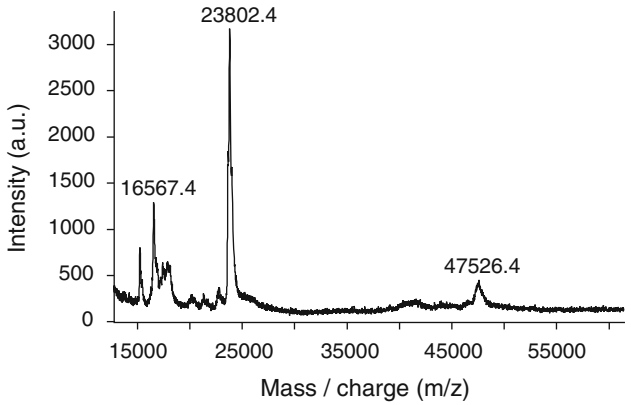

Fig. 5 MALDI-TOF analysis of purified rVif. The mass/charge (m/z) ratio is shown on the x axis, while the y axis displays the signal's intensity in arbitrary units (a.u.)

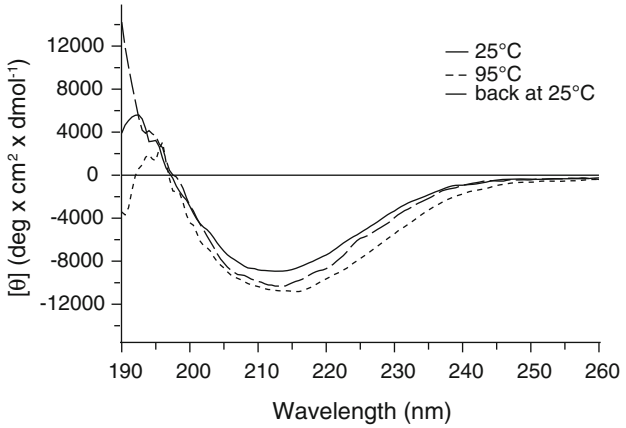

Fig. 6 Far-UV CD analysis of purified rVif. The spectra, recorded at 25, 95 and 25°C after cooling, are expressed as mean residue ellipticities (Θ, y axis) at given wavelengths (nm, x axis)

secondary structure content was calculated with the program CDSSTR (Whitmore and Wallace 2004, 2008). The analysis yielded 11% α-helix, 33% β-sheet, 28% turns and 28% unordered structure. The normalized root mean square difference value of 0.06 demonstrated a good fit between the calculated and the experimentally derived data. These results are in accordance with PsiPred sequence-based predictions (Bryson et al. 2005; Jones 1999), which showed prevalence of β-sheet elements at the N-terminus of the protein and unordered structure interspersed by short α-helixes at the C-terminal portion. The disordered structure of Vifs C-terminal domain has been recently demonstrated by CD and NMR measurements of a chemically synthesized fragment (Reingewertz et al. 2009), as well as by cross-linking and mass spectrometry analysis of an *E. coli*-expressed recombinant Vif (Auclair et al. 2007). Our study is thus the first to report the expression of a complete and folded recombinant Vif protein.

Circular dichroism was further used to evaluate rVifs thermal stability. We used a step-scan procedure in which the sample is heated from 25 to 95°C and spectra are recorded every 5°C. Interestingly, even at 95°C the secondary structure of the protein remained largely intact. The spectrum minimum was maintained at 213–215 nm and negative ellipticity even increased ~2,000 units from 25 to 95°C (Fig. 6). This pattern greatly differs from the changes in CD spectra that usually occur during thermal denaturation, such as significant loss of ellipticity at wavelengths 210–230 nm (α-helix loss) or at 215 nm (β-sheet loss) and concomitant increase in negative ellipticity at 200 nm indicative of random-coil content (Kelly et al. 2005; Sakai-Kato et al. 2008). The results were reproduced in independent measurements and were further verified in a thermal denaturation experiment in which the sample temperature was increased to 95°C on a separate heating block (data not shown). According to these findings, rVif represents a thermostable protein, with a melting temperature (T_m) >95°C.

Recombinant Vif forms soluble high molecular weight aggregates as reported for natural Vif

Chiu et al. (2005) have demonstrated in gel filtration experiments that natural, 293T cell-derived Vif forms high molecular weight aggregates. During SDS-PAGE analysis of the purified recombinant protein, we also observed rVif aggregates of more than 100 kDa, in addition to its appearance as a monomeric protein at the expected molecular weight of 23.7 kDa (Fig. 4b). Therefore, we performed experiments to characterize the aggregation behavior of rVif.

During size exclusion chromatography experiments, it was difficult to elute the protein most likely because of the formation of high molecular weight aggregates.

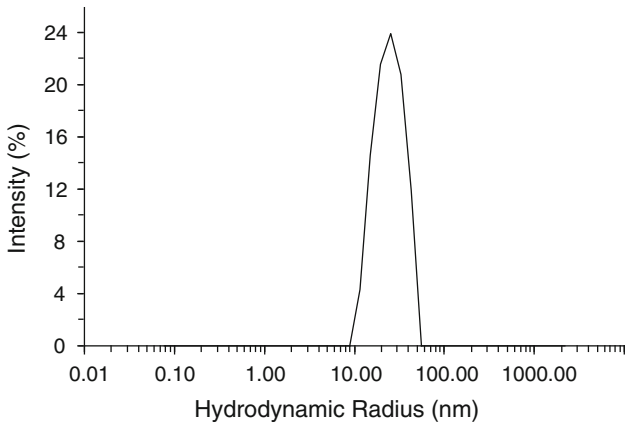

Fig. 7 Dynamic light scattering analysis of purified rVif. Intensity distribution (intensity percentage, *y* axis) calculated from the autocorrelation function of the DLS analysis at a given hydrodynamic radius (nm, *x* axis)

Therefore, we performed DLS measurements which demonstrated that rVif forms large aggregates with a distribution of hydrodynamic radii (R_h) ranging from 10 to 60 nm and most of the protein at 24 nm (Fig. 7). From the width of the distribution, we calculated a degree of polydispersity of 51%. The hydrodynamic radius derived from the maximum of the intensity distribution corresponded to an average molecular weight of 8.0 MDa.

When analyzed by SAXS rVif showed aggregation at three different concentrations (1.36, 0.67 and 0.31 mg/ml). At low resolution the resulting scattering curve did not show the Gaussian shape typical for a mono-disperse spherical protein. Therefore, we could not apply the Guinier approximation to determine the radius of gyration (R_g) and forward scattering I(0). However, using the scattering data of the sample with highest protein concentration, we calculated a pair–distance distribution ($p(r)$) of 29 nm and a maximum particle size (D_{max}) of 80 nm (data not shown). Taken together, these results indicate that rVif retains its natural tendency to self-association.

Conclusion

Our study is the first to provide a protocol for *E. coli* expression and purification of a soluble and folded complete Vif's protein. So far Vifs insoluble properties and low yields in recombinant expression systems have been a major obstacle limiting its use for structural analysis, investigations on Vif's biological functions, diagnostic and therapeutic applications.

rVif produced by us represents a thermostable protein containing mainly β-sheet structural elements and forming high molecular weight aggregates. It may be used to study mechanisms underlying HIV pathogenicity. For example, rVif could be a tool to search for natural ligands and for studies on Vif's binding to known interaction partners, such as APOBEC3G or the regulatory kinases Hck and Fyn. Furthermore, insights may be obtained into the three-dimensional organization of Vif's different domains, such as APOBEC3G/3F binding sites, CZ-box, RNA-binding domain, multimerization and membrane-binding domain. Ultimately, the complete three-dimensional structure of rVif may be obtained by NMR and/or crystallization studies.

Another important application would be the use of recombinant Vif for the characterization of immune responses in HIV-1-infected patients because not much is known about the humoral and cellular responses directed against non-structural HIV proteins. Eventually, rVif may be used to develop new therapeutic strategies for HIV infections.

Acknowledgments This study was supported by a research grant from Biomay, Vienna, Austria (http://www.biomay.com/).

References

Auclair JR, Green KM, Shandilya S, Evans JE, Somasundaran M, Schiffer CA (2007) Mass spectrometry analysis of HIV-1 Vif reveals an increase in ordered structure upon oligomerization in regions necessary for viral infectivity. Proteins 69:270–284

Barraud P, Paillart JC, Marquet R, Tisne C (2008) Advances in the structural understanding of Vif proteins. Curr HIV Res 6:91–99

Bouyac M, Courcoul M, Bertoia G, Baudat Y, Gabuzda D, Blanc D, Chazal N, Boulanger P, Sire J, Vigne R, Spire B (1997) Human immunodeficiency virus type 1 Vif protein binds to the Pr55Gag precursor. J Virol 71:9358–9365

Bryson K, McGuffin LJ, Marsden RL, Ward JJ, Sodhi JS, Jones DT (2005) Protein structure prediction servers at University College London. Nucleic Acids Res 33:W36–W38

Chiu YL, Soros VB, Kreisberg JF, Stopak K, Yonemoto W, Greene WC (2005) Cellular APOBEC3G restricts HIV-1 infection in resting $CD4^+$ T cells. Nature 435:108–114

Deml L, Bojak A, Steck S, Graf M, Wild J, Schirmbeck R, Wolf H, Wagner R (2001) Multiple effects of codon usage optimization on expression and immunogenicity of DNA candidate vaccines encoding the human immunodeficiency virus type 1 Gag protein. J Virol 75:10991–11001

Feng F, Davis A, Lake JA, Carr J, Xia W, Burrell C, Li P (2004) Ring finger protein ZIN interacts with human immunodeficiency virus type 1 Vif. J Virol 78:10574–10581

Gasteiger E, Hoogland C, Gattiker A, Duvaud S, Wilkins MR, Appel RD, Bairoch A (2005) Protein identification and analysis tools on the ExPASy server. In: Walker JM (ed) The proteomics protocols handbook, Humana Press, New Jersey

Goila-Gaur R, Strebel K (2008) HIV-1 Vif, APOBEC, and intrinsic immunity. Retrovirology 5:51

Goncalves J, Jallepalli P, Gabuzda DH (1994) Subcellular localization of the Vif protein of human immunodeficiency virus type 1. J Virol 68:704–712

Haas J, Park EC, Seed B (1996) Codon usage limitation in the expression of HIV-1 envelope glycoprotein. Curr Biol 6:315–324

Holler TP, Foltin SK, Ye QZ, Hupe DJ (1993) HIV1 integrase expressed in *Escherichia coli* from a synthetic gene. Gene 136:323–328

Holmes RK, Malim MH, Bishop KN (2007) APOBEC-mediated viral restriction: not simply editing? Trends Biochem Sci 32:118–128

Jones D (1999) Protein secondary structure prediction based on position-specific scoring matrices. J Mol Biol 292:195–202

Kelly SM, Jess TJ, Price NC (2005) How to study proteins by circular dichroism. Biochim Biophys Acta 1751:119–139

Konarev PV, Volkov VV, Sokolova AV, Koch MHJ, Svergun DI (2003) PRIMUS: a Windows PC-based system for small-angle scattering data analysis. J Appl Crystallogr 36:1277–1282

Kothe DL, Li Y, Decker JM, Bibollet-Ruche F, Zammit KP, Salazar MG, Chen Y, Weng Z, Weaver EA, Gao F, Haynes BF, Shaw GM, Korber BT, Hahn BH (2006) Ancestral and consensus envelope immunogens for HIV-1 subtype C. Virology 352:438–449

Laemmli UK (1970) Cleavage of structural proteins during the assembly of the head of bacteriophage T4. Nature 227:680–685

Leitner T, Foley B, Hahn B, Marx P, McCutchan F, Mellors J, Wolinsky S, Korber B (2005) HIV Sequence Compendium 2005. Theoretical biology and biophysics group, Los Alamos National Laboratory

Malim MH, Emerman M (2008) HIV-1 accessory proteins—ensuring viral survival in a hostile environment. Cell Host Microbe 3:388–398

Nguyen KL, Llano M, Akari H, Miyagi E, Poeschla EM, Strebel K, Bour S (2004) Codon optimization of the HIV-1 vpu and vif genes stabilizes their mRNA and allows for highly efficient rev-independent expression. Virology 319:163–175

Nkolola JP, Essex M (2006) Progress towards an HIV-1 subtype C vaccine. Vaccine 24:391–401

Reingewertz TH, Benyamini H, Lebendiker M, Shalev DE, Friedler A (2009) The C-terminal domain of the HIV-1 Vif protein is natively unfolded in its unbound state. Protein Eng Des Sel 22:281–287

Sakai-Kato K, Ishiguro A, Mikoshiba K, Aruga J, Utsunomiya-Tate N (2008) CD spectra show the relational style between Zic-, Gli-, Glis-zinc finger protein and DNA. Biochim Biophys Acta 1784:1011–1019

Sheehy AM, Gaddis NC, Choi JD, Malim MH (2002) Isolation of a human gene that inhibits HIV-1 infection and is suppressed by the viral Vif protein. Nature 418:646–650

Stanley BJ, Ehrlich ES, Short L, Yu Y, Xiao Z, Yu XF, Xiong Y (2008) Structural insight into the human immunodeficiency virus Vif SOCS box and its role in human E3 ubiquitin ligase assembly. J Virol 82:8656–8663

Svergun DI (1992) Determination of the regularization parameter in indirect-transform methods using perceptual criteria. J Appl Cryst 25:495–503

Taylor BS, Hammer SM (2008) The challenge of HIV-1 subtype diversity. N Engl J Med 359:1965–1966

Towbin H, Staehelin T, Gordon J (1979) Electrophoretic transfer of proteins from polyacrylamide gels to nitrocellulose sheets: procedure and some applications. Proc Natl Acad Sci USA 76:4350–4354

UNAIDS (2008) Report on the global HIV/AIDS epidemic 2008: executive summary. UNAIDS/08.27E/JC1511E. WHO Library Cataloguing, in-Publication Data

Whitmore L, Wallace BA (2004) DICHROWEB, an online server for protein secondary structure analyses from circular dichroism spectroscopic data. Nucleic Acids Res 32:W668–W673

Whitmore L, Wallace BA (2008) Protein secondary structure analyses from circular dichroism spectroscopy: methods and reference databases. Biopolymers 89:392–400

Yang X, Goncalves J, Gabuzda D (1996) Phosphorylation of Vif and its role in HIV-1 replication. J Biol Chem 271:10121–10129

Yang S, Sun Y, Zhang H (2001) The multimerization of human immunodeficiency virus type I Vif protein: a requirement for Vif function in the viral life cycle. J Biol Chem 276:4889–4893